Electron Hopping and Charge Separation within a Naphthalene-1,4:5,8-bis(dicarboximide) Chiral Covalent Organic Cage

Tomas Solomek, Natalia E. Powers-Riggs, Yi-Lin Wu, Ryan M. Young, Matthew D. Krzyaniak, Noah E. Horwitz, and Michael R. Wasielewski*

Department of Chemistry and Argonne-Northwestern Solar Energy Research (ANSER) Center, Northwestern University, Evanston, Illinois 60208-3113, United States

* Supporting Information

ABSTRACT: We present the stereoselective synthesis of a chiral covalent organic cage consisting of three redox-active naphthalene-1,4:5,8-bis(dicarboximide) (NDI) units by dynamic imine chemistry. Single crystal X-ray diffraction analysis shows that host−guest interactions and racemic cocrystallization allow for controlling the solid state structure. Electronic interactions between the NDI units probed by absorption and circular dichroism spectroscopies, electrochemistry and theoretical calculations are shown to be weak. Photoexcitation of NDI leads to intracage charge separation with a longer lifetime than observed in the corresponding monomeric NDI and dimeric NDI cyclophane imines. The EPR spectrum of the singly reduced cage shows that the electron is localized on a single NDI unit at ambient temperatures and transitions to rapid hopping among all three NDI units upon heating to 350 K. Dynamic covalent chemistry thus promises rapid access to covalent organic cages with well-defined architectures to study charge accumulation and electron transport phenomena.

Thermodynamically driven condensation of multifunctional amines and aldehydes, known as dynamic imine chemistry,[1] has proved to be a powerful method for the construction of macrocyclic compounds,[2] rotaxanes,[3] catenanes,[4] covalent organic cages (COCs),[5] covalent organic frameworks[6] (COFs) and exotic molecules such as Borromean rings[7] and Solomon knots.[8] The type of product is dictated mainly by the number of functional groups in the amine and the aldehyde, the angle between these functional groups, and the catalyst used.[1] Condensation of diamines with trialdehydes often results in the formation of COC imines that exhibit interesting guest binding and gas sorption properties.[5b,d] COC imines are relatively rigid, possess high symmetry and, unlike COFs, can easily be processed to fabricate thin films as demonstrated by molecular-sieving membranes for selective gas separation.[5d]

At the same time, the molecular units in COCs are spatially arranged with high precision. Such well-defined molecular architectures are of paramount importance in understanding electronic communication between chromophores and redox partners.[9] COCs are thus appealing building blocks of photo/redox-active materials for organic electronics. However, despite the rapidly developing field of molecular nanobelts/nanohoops based on porphyrins,[10] extended viologens,[11] rylene dyes[12] and aromatic hydrocarbons,[13] related cage systems[14] remain largely unexplored apart from the ubiquitous fullerenes.[15] Moreover, unlike in coordination cages,[16] the possibility of through-space electron transfer within a covalent all-organic cage has not been demonstrated to date. We therefore envisioned synthesizing a COC with multiple redox-active naphthalene-1,4:5,8-bis-(dicarboximide) (NDI) chromophores[17] by means of dynamic imine chemistry. If such a strategy proved successful, it could allow for rapid access to new organic materials.

We designed COC 1[18] (Scheme 1) as a [3+2] condensation product and we evaluated the strain (Scheme S1, Table S1) that accompanies its formation and that of related cyclophane 2 reported previously.[2] We found that the intermediate strain in 1 (~15 kcal mol^{-1} for 1; ~5 kcal mol^{-1} for 2) should allow for its synthesis by water removal. Both enantiomers of COC imine 1,

Scheme 1. Synthesis of 1−3[15]

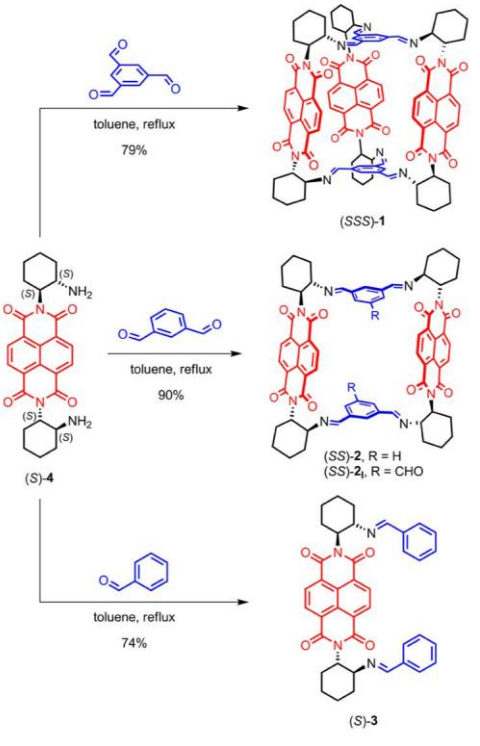

cyclophane 2 and a reference compound 3 were therefore synthesized by condensation of an appropriate aldehyde and chiral NDI diamine 4, prepared from enantiomerically pure trans-1,2-diaminocyclohexane and naphthalene-1,4:5,8-dicarboxydianhydride (Scheme S2), in toluene under Dean–Stark conditions. Imines 1–3 are stable in CH_2Cl_2 or THF solutions for days, but hydrolyze readily on the surface of silica or alumina (1 is the most and 3 is the least stable in the series). The compounds were therefore purified by precipitation from their toluene solutions with methanol in good yields and purity. Their structures were confirmed by ^{1}H, ^{13}C and 2D homo- and heteronuclear correlation NMR spectroscopy and HR-ESI-ToF mass spec-trometry (Figures S1–S27). All ^{1}H and ^{13}C NMR resonances of cage 1 were fully assigned (Figure S10).

The equilibrium nature of the dynamic imine chemistry allowed us to investigate the mechanism of cage 1 formation in more detail. Condensation of a substoichiometric amount of 4 with 1,3,5-triformylbenzene, provided, besides 1, a new compound with ^{1}H NMR spectrum suggesting that the new compound is a [2+2] condensation product. Partial hydrolysis of 1 on a short silica column gave a product with an identical ^{1}H NMR spectrum (Figures S28–S30). We therefore assigned the spectrum to cyclophane 2_I (Scheme 1) as an intermediate in the formation of cage 1.

The [2+2] condensation of isophthalaldehyde with a racemate of 4 yielded a mixture of (RR)- and (RS)-2 diastereomers in ~2:1 ratio (see Figure S31) in agreement with our DFT calculations (Table S2) that show that (RR)-2 is more stable than (RS)-2. The stereoselectivity reinforces itself in the case of [3+2] condensation. Only the signals of homochiral 1 could be observed in the ^{1}H NMR spectrum of the reaction mixture, although a ratio (RRR)-1/(RRS)-1 of 1:3 is expected if the reaction is statistical. Formation of cage 1 is therefore highly stereoselective in agreement with our calculations.

The gas phase DFT model predicts that cage 1 possesses high symmetry (D_3 point group) in accord with its simple ^{1}H NMR spectrum and has a large internal cavity that can be occupied by guest molecules. Indeed, a satisfactory fit to data obtained by small-angle X-ray scattering of a THF solution of 1 (Figures S36–S39) required a model with three THF molecules inside the cavity of 1. Definitive proof for the presence of solvent guests was provided by X-ray diffraction (Figures 1 and S40–S45) of a single crystal grown by methanol vapor diffusion into a toluene solution of 1 (Figure 1a; $P2_1$ space group). Two crystallographically distinct cages of 1 were found in the crystal structure: one with two and one with three highly ordered toluene molecules inside the cage, each within van der Waals contact with the π–acidic surface[19] of an NDI. This donor–acceptor interaction determines the packing of 1 in the solid because it prevents close contact of the cages and limits the edge-to-face interactions between NDIs to two per cage. As proof, we crystallized 1 from nitrobenzene, an electron-deficient molecule of comparable size to toluene, and found no ordered nitrobenzene molecules in the cavity of 1. As a consequence of more free space, four edge-to-face interactions per cage are allowed in the solid 1 superstructure (Figure 1b; $C222_1$), which is more ordered. We also succeeded in determining the crystal structure (Figure S45) of the racemic mixture of 1 with a centrosymmetric unit cell ($P\bar{1}$), which demonstrates the ability to control the solid state morphology by host–guest interactions or blends of stereoisomers.

The UV–vis absorption spectra of 1–3 are very similar except for the molar absorption coefficient of the NDI absorption band (λ_{max}), which nearly doubles for 2 when compared to 3. The

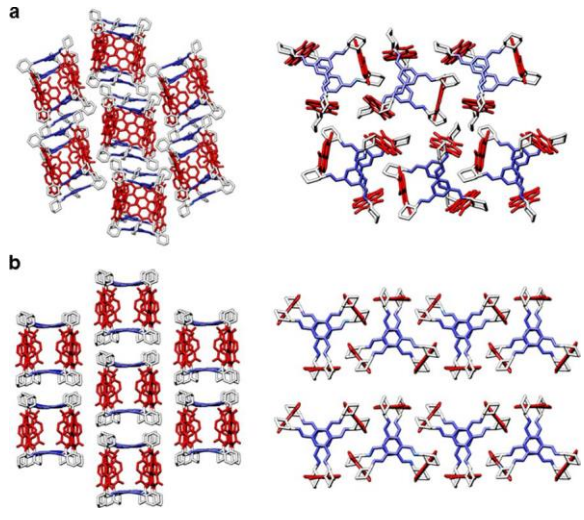

Figure 1. Solid-state (super)structures (sideview, left; topview, right) of a single crystal of 1 grown from (a) toluene and (b) nitrobenzene. NDI, red; cyclohex-1,2-diyl, white; aromatic imine, blue.

addition of the third NDI chromophore in 1 does not increase λ_{max} considerably as a result of spatially coupled transition dipole moments.[20] In addition, theory predicts that exciton coupling of the three NDI chromophores in 1 should result in a formally forbidden electronic transition to a doubly degenerate lowest singlet excited state.[20] The absorption spectrum of 1 displays a weak shoulder (Figure 2 and Figure S46), which is absent in 3 and

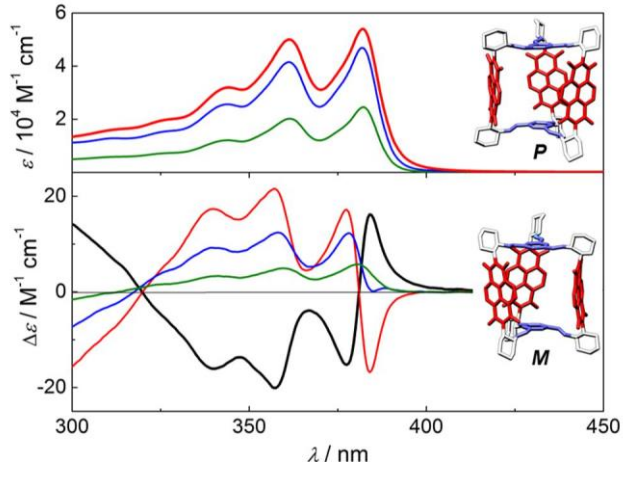

Figure 2. Absorption (top) and circular dichroism (bottom) spectra of (RRR)-1 (M-, black), (SSS)-1 (P-, red), (SS)-2 (blue) and (S)-3 (olive) in CH_2Cl_2.

is slightly red-shifted relative to the major absorption band in agreement with TD-DFT calculations (Table S3) indicating that this transition is weakly allowed.

The strain in 1 induces a helical twist[21] of the NDI units that can be observed in the crystal structure and the DFT model. The (RRR)-1 and the (SSS)-1 enantiomers possess M- and P-helicity, respectively, and exhibit a strong positive and negative Cotton effect in their circular dichroism spectra (Figures 2 and S47–S50). The exciton coupling in 2 is considerably smaller than in 1 due to lower strain causing a smaller helical twist.

Cyclic and differential pulse voltammetry (Figures S51–S57) of 1–3 showed only two reduction waves characteristic of $NDI^{\bullet-}$ and NDI^{2-} suggesting that the electronic coupling between the

NDI units in 1 and 2 is small. Chronoamperometry experiments (Figure S58) confirmed that each reduction wave consists of a three-electron process in 1. Such minimal Coulombic penalty makes the nanometer-sized cage 1 an appealing all-organic 6-electron acceptor.[12b,d]

It is known that the lowest excited singlet state of NDI (^{1}*NDI) is a strong oxidant capable of removing an electron from aryl groups attached to the imide position,[22] which may be useful for redox catalysis or organic electronics. We were therefore interested in the effect of the more constrained geometry of 1 on the charge separated (CS) state lifetime. Following photoexcitation of 1−3 in CH_2Cl_2 (~10^{-4} M) with a 350 nm, 100 fs laser pulse, femtosecond transient absorption (fsTA) spectroscopy showed (Figure 3; also section H in the SI) that initial

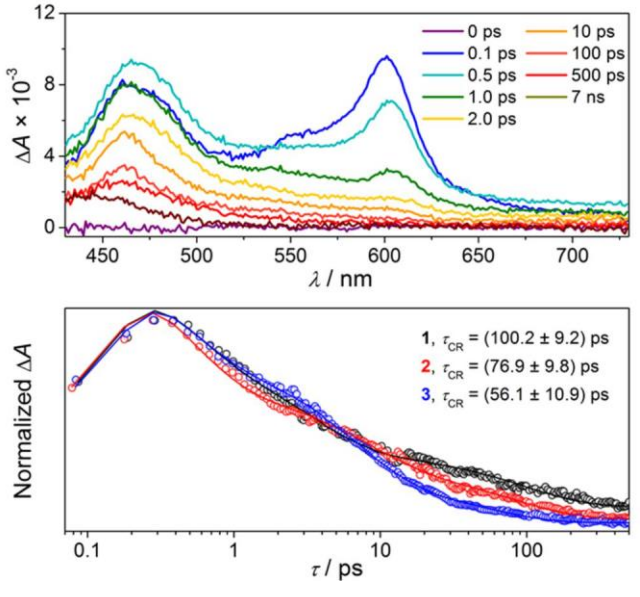

Figure 3. Femtosecond transient absorption spectra of 1 in CH_2Cl_2 at 298 K following a 350 nm laser pulse (0.6 μJ/pulse) excitation (top) and kinetic traces (470 nm) with associated fit (see text) for 1−3 (bottom). Lifetimes of charge recombination (τ_{CR}) are shown.

formation of ^{1}*NDI (λ_{max} = 603 and 470 nm) is followed by rapid oxidation of the aromatic imine bridge (τ_{CS} = 0.4−0.6 ps). Formation of the NDI$^{\bullet-}$ radical anion[23] (λ_{max} = 470, 530 and 610 nm) is followed by fast solvent relaxation (τ_{rlx} = 4−6 ps). The radical ion pair then rapidly charge recombines (CR), where τ_{CR} = 100.2 ± 9.2, 76.9 ± 9.8 and 56.1 ± 10.9 ps for 1, 2 and 3, respectively, to form the NDI triplet state (^{3}*NDI) that persists for microseconds. ^{3}*NDI is most likely produced by the spin−orbit charge transfer mechanism because the π systems of the imine donor and the NDI acceptor are nearly orthogonal.[24] Raising the radical ion pair energy by placing 1 in nonpolar dioxane accelerates CR (τ_{CR} = 84 ps, Table S8, Figures S65 and S66); thus indicating that CR occurs in the Marcus normal region, which is consistent with charge recombination primarily to ^{3}*NDI rather than the NDI singlet ground state, which is expected to lie in the Marcus inverted region.[22] The quantum yield of ^{3}*NDI formation was, however, not determined. The data suggest that the more rigid structure of 1 increases the CS state lifetime either by increasing the internal reorganization energy or restraining 1 from exploring the parts of energy surface with optimal electronic coupling for CR.

The short CR lifetime did not allow us to observe the radical ion pair within the COC by time-resolved EPR spectroscopy. Thus, we performed continuous-wave (CW) EPR experiments on 1−3 (DMF, 5 × 10^{-4} M) chemically reduced with cobaltocene (0.1−0.9 equiv) to observe whether the electron can hop rapidly among multiple weakly coupled NDI units. According to the McConnell relationship,[25] the isotropic hyperfine coupling decreases linearly with the number of equivalent nuclei on which the unpaired spin density resides on the time scale of the EPR experiment. Figure 4 shows the CW-EPR spectra of 1$^{\bullet-}$ and

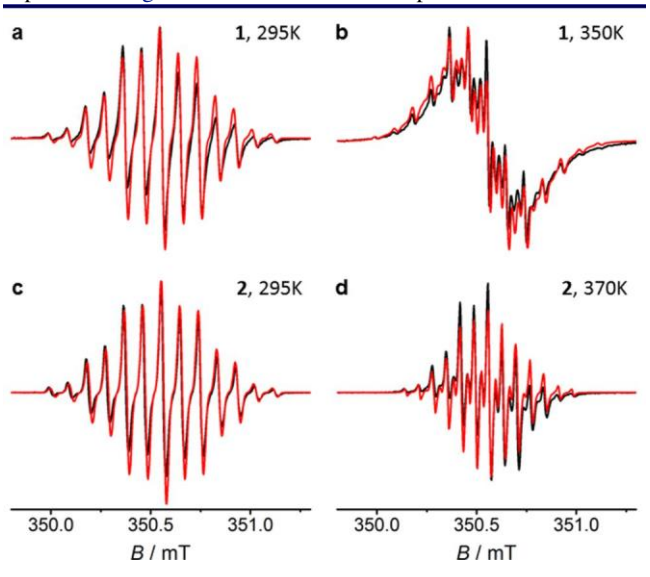

Figure 4. CW-EPR spectra of 1 (a, b) and 2 (c, d) at room and elevated temperatures. Overlay of the experimental (black) and the simulated spectra (see text).

2$^{\bullet-}$ at ambient and elevated temperatures. The experimental and simulated spectra of 1$^{\bullet-}$ and 2 $^{\bullet-}$ at 295 K are similar to that of 3$^{\bullet-}$ (Figure S67), which clearly shows that the electron is localized on a single NDI. The average NDI-NDI distance in 1 is large (9.9 Å; Figure S41), and therefore hinders electron hopping between the NDI units on the EPR time scale at 295 K due to weak electronic coupling, consistent with what we observed in our electrochemistry and UV absorption experiments, as well as the 0.17 eV internal reorganization energy for NDI reduction to NDI$^{\bullet-}$ determined using DFT calculations.[26] In contrast, raising the temperature of 1$^{\bullet-}$ and 2$^{\bullet-}$ to 350 and 370 K, respectively, results in the appearance of a second set of narrow lines, which is more prominent for 1$^{\bullet-}$ than 2$^{\bullet-}$. The narrow line EPR spectra of 1$^{\bullet-}$ and 2$^{\bullet-}$ are readily fit to two species (see Section I in the SI for further details). All observed species for both 1$^{\bullet-}$ and 2$^{\bullet-}$ possess nearly identical g-factors irrespective of temperature, whereas the hyperfine coupling constants of the second narrow line width species that appear in the high temperature data are one-third those of 1$^{\bullet-}$ and one-half those of 2$^{\bullet-}$ at 295 K. This demonstrates that at 350 K, the electron is hopping among all three NDI redox units in 1$^{\bullet-}$ and between both units in 2$^{\bullet-}$ at 370 K, spending, on average, an equal time on each NDI. Moreover, the different hyperfine couplings for 1$^{\bullet-}$ and 2$^{\bullet-}$ suggest that the species observed at elevated temperatures does not arise from bimolecular electron transfer, which is presumably the origin of EPR spectra line broadening at elevated temperature when more than a 10-fold increase in the concentration of neutral 1 in the solution is used (Figure S68). The EPR spectra of 1$^{\bullet-}$ and 2$^{\bullet-}$ were additionally fit with an intramolecular exchange model of Heinzer[27] (Figure S69) that provided us with the approximate rate constants of the intramolecular electron transfer. Although

the electron hopping occurs with a $k \sim 10^5\ s^{-1}$, a lower limit of EPR time resolution, at room temperature, it accelerates by nearly 2 orders of magnitude to $k \sim 8 \times 10^6\ s^{-1}$ by increasing the temperature for $1^{\bullet-}$ and $2^{\bullet-}$ at 350 and 370 K, respectively.

In summary, we have reported on electron hopping and charge separation within a chiral covalent organic cage assembled by dynamic imine chemistry that demonstrates the potential to access rapidly a new class of organic cage molecules with interesting optoelectronic properties. These could prove useful in enantioselective molecular recognition, multielectron accumulation for catalysis, organic electronics and sensing.

ASSOCIATED CONTENT

* Supporting Information

Experimental procedures, spectra of compounds, exper-imental and computational details (PDF)
CCDC 1525640 (CIF)
CCDC 1525641 (CIF)
CCDC 1525642 (CIF)

AUTHOR INFORMATION

Corresponding Author
*m-wasielewski@northwestern.edu
ORCID
Ryan M. Young: 0000-0002-5108-0261
Michael R. Wasielewski: 0000-0003-2920-5440

Notes

The authors declare no competing financial interest.

ACKNOWLEDGMENTS

This work was supported by the Chemical Sciences, Geosciences, and Biosciences Division, Office of Basic Energy Sciences, DOE under grant no. DE-FG02-99ER14999. We thank Dr. Saman Shafaie for collecting high-resolution mass spectrometric data. T.S.thanks the Swiss National Science Foundation for postdoctoral scholarship.

REFERENCES

(1) Belowich, M. E.; Stoddart, J. F. Chem. Soc. Rev. 2012, 41, 2003.
(2) Kaik, M.; Gawronski, J. Org. Lett. 2006, 8, 2921.
(3) (a) Cantrill, S. J.; Rowan, S. J.; Stoddart, J. F. Org. Lett. 1999, 1, 1363. (b) Glink, P. T.; Oliva, A. I.; Stoddart, J. F.; White, A. J. P.; Williams, D. J. Angew. Chem., Int. Ed. 2001, 40, 1870.
(4) Koshkakaryan, G.; Cao, D.; Klivansky, L. M.; Teat, S. J.; Tran, J. L.; Liu, Y. Org. Lett. 2010, 12, 1528.
(5) (a) Xu, D.; Warmuth, R. J. Am. Chem. Soc. 2008, 130, 7520. (b) Tozawa, T.; Jones, J. T. A.; Swamy, S. I.; Jiang, S.; Adams, D. J.; Shakespeare, S.; Clowes, R.; Bradshaw, D.; Hasell, T.; Chong, S. Y.; Tang, C.; Thompson, S.; Parker, J.; Trewin, A.; Bacsa, J.; Slawin, A. M. Z.; Steiner, A.; Cooper, A. I. Nat. Mater. 2009, 8, 973. (c) Hasell, T.; Wu, X. F.; Jones, J. T. A.; Bacsa, J.; Steiner, A.; Mitra, T.; Trewin, A.; Adams, D. J.; Cooper, A. I. Nat. Chem. 2010, 2, 750. (d) Song, Q. L.; Jiang, S.; Hasell, T.; Liu, M.; Sun, S. J.; Cheetham, A. K.; Sivaniah, E.; Cooper, A. I. Adv. Mater. 2016, 28, 2629. (e) Zhang, G.; Mastalerz, M. Chem. Soc. Rev. 2014, 43, 1934.
(6) (a) Uribe-Romo, F. J.; Hunt, J. R.; Furukawa, H.; Klock, C.; O'Keeffe, M.; Yaghi, O. M. J. Am. Chem. Soc. 2009, 131, 4570. (b) Uribe-Romo, F. J.; Doonan, C. J.; Furukawa, H.; Oisaki, K.; Yaghi, O. M. J. Am. Chem. Soc. 2011, 133, 11478.
(7) Chichak, K. S.; Cantrill, S. J.; Pease, A. R.; Chiu, S. H.; Cave, G. W. V.; Atwood, J. L.; Stoddart, J. F. Science 2004, 304, 1308.
(8) Pentecost, C. D.; Chichak, K. S.; Peters, A. J.; Cave, G. W. V.; Cantrill, S. J.; Stoddart, J. F. Angew. Chem., Int. Ed. 2007, 46, 218.
(9) Wasielewski, M. R. Chem. Rev. 1992, 92, 435.
(10) (a) Hoffmann, M.; Karnbratt, J.; Chang, M. H.; Herz, L. M.; Albinsson, B.; Anderson, H. L. Angew. Chem., Int. Ed. 2008, 47, 4993. (b) Sprafke, J. K.; Kondratuk, D. V.; Wykes, M.; Thompson, A. L.; Hoffmann, M.; Drevinskas, R.; Chen, W. H.; Yong, C. K.; Karnbratt, J.; Bullock, J. E.; Malfois, M.; Wasielewski, M. R.; Albinsson, B.; Herz, L. M.; Zigmantas, D.; Beljonne, D.; Anderson, H. L. J. Am. Chem. Soc. 2011, 133, 17262. (c) Kondratuk, D. V.; Perdigao, L. A.; Esmail, A. M. S.; O'Shea, J. N.; Beton, P. H.; Anderson, H. L. Nat. Chem. 2015, 7, 317.
(11) Dale, E. J.; Vermeulen, N. A.; Juricek, M.; Barnes, J. C.; Young, R. M.; Wasielewski, M. R.; Stoddart, J. F. Acc. Chem. Res. 2016, 49, 262.
(12) (a) Schneebeli, S. T.; Frasconi, M.; Liu, Z. C.; Wu, Y. L.; Gardner, D. M.; Strutt, N. L.; Cheng, C. Y.; Carmieli, R.; Wasielewski, M. R.; Stoddart, J. F. Angew. Chem., Int. Ed. 2013, 52, 13100. (b) Wu, Y. L.; Nalluri, S. K. M.; Young, R. M.; Krzyaniak, M. D.; Margulies, E. A.; Stoddart, J. F.; Wasielewski, M. R. Angew. Chem., Int. Ed. 2015, 54, 11971. (c) Wu, Y. L.; Young, R. M.; Frasconi, M.; Schneebeli, S. T.; Spenst, P.; Gardner, D. M.; Brown, K. E.; Wu¨rthner, F.; Stoddart, J. F.; Wasielewski, M. R. J. Am. Chem. Soc. 2015, 137, 13236. (d) Nalluri, S. K. M.; Liu, Z. C.; Wu, Y. L.; Hermann, K. R.; Samanta, A.; Kim, D. J.; Krzyaniak, M. D.; Wasielewski, M. R.; Stoddart, J. F. J. Am. Chem. Soc. 2016, 138, 5968.
(13) Lewis, S. E. Chem. Soc. Rev. 2015, 44, 2221.
(14) (a) Durot, S.; Taesch, J.; Heitz, V. Chem. Rev. 2014, 114, 8542. (b) Matsui, K.; Segawa, Y.; Itami, K. J. Am. Chem. Soc. 2014, 136, 16452.
(15) (a) Kirner, S.; Sekita, M.; Guldi, D. M. Adv. Mater. 2014, 26, 1482. (b) Kawashima, Y.; Ohkubo, K.; Fukuzumi, S. Chem. - Asian J. 2015, 10, 44.
(16) (a) Furutani, Y.; Kandori, H.; Kawano, M.; Nakabayashi, K.; Yoshizawa, M.; Fujita, M. J. Am. Chem. Soc. 2009, 131, 4764. (b) Mahata, K.; Frischmann, P. D.; Wu¨rthner, F. J. Am. Chem. Soc. 2013, 135, 15656. (c) Frank, M.; Ahrens, J.; Bejenke, I.; Krick, M.; Schwarzer, D.; Clever, G. H. J. Am. Chem. Soc. 2016, 138, 8279.
(17) Al Kobaisi, M.; Bhosale, S. V.; Latham, K.; Raynor, A. M.; Bhosale, S. V. Chem. Rev. 2016, 116, 11685.
(18) We abbreviate the (S,S,S,S,S,S,S,S,S,S,S,S)-enantiomer of 1 as (SSS)-1, because the precursor diamine 4 is synthesized from enantiomerically pure trans-1,2-cyclohexanediamine. Accordingly, the same nomenclature is used for 2, 3 and 4 (see SI for further details).
(19) Gorteau, V.; Bollot, G.; Mareda, J.; Perez-Velasco, A.; Matile, S. J. Am. Chem. Soc. 2006, 128, 14788.
(20) Kasha, M.; Rawls, H. R.; El-Bayoumi, M. A. Pure Appl. Chem. 1965, 11, 371.
(21) Rickhaus, M.; Mayor, M.; Juricek, M. Chem. Soc. Rev. 2016, 45, 1542.
(22) Ganesan, P.; Baggerman, J.; Zhang, H.; Sudholter, E. J. R.; Zuilhof, H. J. Phys. Chem. A 2007, 111, 6151.
(23) Gosztola, D.; Niemczyk, M. P.; Svec, W.; Lukas, A. S.; Wasielewski, M. R. J. Phys. Chem. A 2000, 104, 6545.
(24) (a) Okada, T.; Karaki, I.; Matsuzawa, E.; Mataga, N.; Sakata, Y.; Misumi, S. J. Phys. Chem. 1981, 85, 3957. (b) Dance, Z. E. X.; Mickley, S. M.; Wilson, T. M.; Ricks, A. B.; Scott, A. M.; Ratner, M. A.; Wasielewski, M. R. J. Phys. Chem. A 2008, 112, 4194.
(25) (a) McConnell, H. M. J. Chem. Phys. 1956, 24, 632. (b) McConnell, H. M. J. Chem. Phys. 1956, 24, 764.
(26) Scott, A. M.; Miura, T.; Ricks, A. B.; Dance, Z. E. X.; Giacobbe, E. M.; Colvin, M. T.; Wasielewski, M. R. J. Am. Chem. Soc. 2009, 131, 17655.
(27) (a) Heinzer, J. Mol. Phys. 1971, 22, 167. (b) Zalibera, M.; Jalilov, A. S.; Stoll, S.; Guzei, I. A.; Gescheidt, G.; Nelsen, S. F. J. Phys. Chem. A 2013, 117, 1439.